Structural Engineering and Mechanics, *Vol. 72, No. 4 (2019) 491-502*
DOI: https://doi.org/10.12989/sem.2019.72.4.491

Accurate buckling analysis of rectangular thin plates by double finite sine integral transform method

Salamat Ullah[a], Jinghui Zhang* and Yang Zhong[b]

Faculty of Infrastructure Engineering, Dalian University of Technology, No.2 Linggong Road, Ganjingzi District, Dalian City, Liaoning Province, P.R.C., 116024, China

(Received April 10, 2019, Revised June 10, 2019, Accepted June 12, 2019)

Abstract. This paper explores the analytical buckling solution of rectangular thin plates by the finite integral transform method. Although several analytical and numerical developments have been made, a benchmark analytical solution is still very few due to the mathematical complexity of solving high order partial differential equations. In solution procedure, the governing high order partial differential equation with specified boundary conditions is converted into a system of linear algebraic equations and the analytical solution is obtained classically. The primary advantage of the present method is its simplicity and generality and does not need to pre-determine the deflection function which makes the solving procedure much reasonable. Another advantage of the method is that the analytical solutions obtained converge rapidly due to utilization of the sum functions. The application of the method is extensive and can also handle moderately thick and thick elastic plates as well as bending and vibration problems. The present results are validated by extensive numerical comparison with the FEA using (ABAQUS) software and the existing analytical solutions which show satisfactory agreement.

Keywords: double finite sine integral transform method; buckling analysis; analytical solution; rectangular thin plate

1. Introduction

Plate is an important structure element in many engineering applications due to its key role as load bearing component. Representative practical examples include rigid pavements, building floor and roof, bridge deck, aircraft wings, wallboard of the launch vehicles, etc. The buckling problem of such structures causes reduction in structure stiffness, as a result reducing its load carrying capacity. Therefore, these structures must endure enough compressive forces such that buckling of the structures, which may cause premature failure, is avoided. This underscores the importance of understanding the performance and capacities of plates and further guiding the design of related engineering devices and structures. Hence, the buckling characteristics of plates need to be studied in order to develop an accurate and reliable design. In addition, the buckling solutions of higher order partial differential equations (PDE) are few, and the solving process is much more difficult than the present method. By the proposed analytical solution, the exact buckling solutions of the plate are obtained, which can be confidently used as a benchmark solution for the validation of other methods.

Numerous methods have been proposed to solve buckling problems of plates in the past few decades. Here we briefly reviewed some of the latest numerical developments in this field. The finite difference method is commonly used methods due to its simplicity and high versatility and has been utilized to obtain the approximate buckling solution of nanoplates *(*Karamooz Ravari *et al.* 2014, Karamooz Ravari and Shahidi 2013). The buckling characteristics of thin plates are analyzed by differential quadrature method (Jiang *et al.* 2008, Wang *et al.* 2003, Wang and Huang 2009). The free vibration of the rectangular thick plate with point support is studied by introducing two-dimensional basic functions to describe the variation of three-dimensional displacement in a thin layer by finite layer method Zhou *et al.* (2000). The same method is utilized to investigate the three-dimensional dynamic response of functionally graded carbon nanotubes Wu and Lin (2015). The discrete singular convolution method is employed to examine the buckling problem of plate, the method is simple, which proves the applicability of the method to be used for such problems because of its simplicity (Civalek *et al.* 2010, Civalek and Yavas 2008). A meshless method is adopted to obtain the buckling solutions of composite laminated plates Wang *et al.* (2002), and Reissner–Mindlin plates subjected to in-plane edge loads Bui *et al.* (2011). A novel meshfree method is utilized to solve buckling and vibration problems of composite plates Bui and Nguyen (2011), and composite laminates under in-plane compression loading Bui (2011). Taking into account the minimum total energy variational principle the vibration behavior of stepped plates are studied by extended Kantorovich method Singhatanadgid and Taranajetsada (2016). An exact finite strip method is used to find the buckling solution of a moderately thick plate by considering first order shear deformation theory (Ghannadpour and Ovesy 2009, Ovesy *et al.* 2013). In addition, the FEM

*Corresponding author, Ph.D. Student
E-mail: zhangjinghui653@mail.dlut.edu.cn
[a] Ph.D. Student
[b] Ph.D. Professor

ISSN: 1225-4568 (Print), 1598-6217 (Online)

(Adany *et al.* 2018, Jeyaraj 2013, Komur and Sonmez 2015) and Ritz energy method (Huang *et al.* 2019, Lau and Hancock 1986, Mahendran and Murray 1986, Mijušković *et al.* 2015) have been applied to study the buckling and of various plate structures.

The above method meets the engineering requirements, but an approximate solution is obtained, which is the main disadvantage of the numerical methods. Therefore, a benchmark analytical solution is still required for validation of other analytical and approximate methods. On the other hand, analytical solution of a plate is available for some specific boundary conditions, such as a plate with all edges simply supported or plate with two opposite edges simply supported, which is called Lévy-type solution. Using this approach the buckling solutions of rectangular plate subjected to uniaxial and intermediate loads are obtained (Xiang et al. 2003). The first attempt is made on the basis of the superposition method Timoshenko S.P.(1961), it provides many exact solutions, but working in the semi-inverse method which needs trial functions to fulfill the boundary conditions, which do not always exist. A symplectic superposition method is applied for the buckling (Li *et al.* 2018, Wang *et al.* 2016) bending (Li *et al.* 2014, Liu and Li 2010) and free vibration (Li *et al.* 2015, 2016) analysis of rectangular thin plates, which is the combination of the superposition method and symplectic elasticity approach (Lim *et al.* 2007, 2009, Lim and Xu 2010) applied successfully to solve elastic plate problems. A closed-form solution (Liu and Xing 2011, Yufeng Xing and Zekun Wang 2017) and separation of variable method (Liu *et al.* 2014, Xing and Liu 2009) is effectively implemented to obtain the exact free vibration solution of rectangular plates. Recently, two-dimensional generalized integral transform method is employed to determine the analytical bending and buckling solutions of rectangular thin plates (Ullah *et al.* 2019, Zhang *et al.* 2018).

Although many important achievements have been made, the research in this field is still vigorous. Researchers are looking for new analytical techniques to solve complex plate buckling problems because of its practical needs. In recent years, the finite integral transformation is efficiently implemented in solving partial differential equations, which provides a piece of new knowledge for analytical plate solutions. This method is utilized to the vibration and bending problems of plate with a class of complex boundary value problems (BVPs) (Li *et al.* 2009, Tian *et al.* 2011, 2015, Zhang and Xu 2017, 2018, Zhang and Zhang 2018, Zhong *et al.* 2014, Zhong and Yin 2008). The advantage of the integral transform method is that it is simple and general and can handle other elastic plate problems. However, there have been no reports available, to the best of our knowledge, by using finite integral transformation for buckling analysis of rectangular thin plates.

This study presents double finite sine integral transformation to analytically solving the buckling problems of rectangular thin plates, focus on typical non-Lévy-type plates. The buckling governing PDEs for thin plates are converted into a system of linear algebraic equations. Then, through the existence of non-zero solutions in the equations, the buckling solution can be easily determined. The analytical solutions are obtained for different boundary conditions and aspect ratios subjected to uniaxial compressive loads which are believed to provide benchmark solution for validation of other methods. The validity of the method is verified by the good consistency with the existing analytical solutions and the finite element analysis (FEA) using (ABAQUS) software.

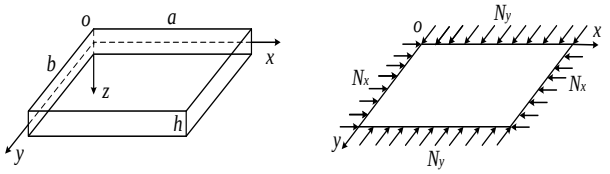

(a) a thin plate

(b) the plate under biaxial compression along *x* and *y* direction

Fig. 1 Schematic illustration of a thin plate the plate under biaxial compression along *x* and *y* direction

2. Application of finite integral transformation for the buckling analysis of rectangular thin plates

Considering the rectangular thin plate with length *a*, width *b* and uniform thickness *h*, the coordinate system is shown in Fig. 1.

According to the classical Kirchhoff plate theory the buckling equation of thin plate subjected to normal loads N_x and N_y with uniformly distributed along *x* and *y* directions can be expressed as Timoshenko S.P.(1961)

$$\frac{\partial^4 W}{\partial x^4}+2\frac{\partial^4 W}{\partial x^2\partial y^2}+\frac{\partial^4 W}{\partial y^4}+\frac{N_x}{D}\frac{\partial^2 W}{\partial x^2}+\frac{N_y}{D}\frac{\partial^2 W}{\partial y^2}=0 \tag{1}$$

Where $D=Eh^3/12(1-\mu^2)$ is the flexural rigidity of plate, in which E is the Young's modulus and μ is Poisson's ratios of plate respectively. $W(x,y)$ is the out-of-plane displacement and is a function of independent variables *x* and *y* defined within a rectangular domain $0\le x\le a$ and $0\le y\le b$. The finite sine integral transformation is defined as

$$W_{mn}=\int_0^a\int_0^b W(x,y)\sin(\alpha_m x)\sin(\beta_n y)\mathrm{d}x\mathrm{d}y \tag{2}$$

The inversion is expressed as

$$W(x,y)=\frac{4}{ab}\sum_{m=1}^{\infty}\sum_{n=1}^{\infty}W_{mn}\sin(\alpha_m x)\sin(\beta_n y) \tag{3}$$

where $\alpha_m=m\pi/a$; $\beta_n=n\pi/b$.

The high order partial derivatives of $W(x,y)$ in Eq. (1) are derived as

$$\begin{aligned}&\int_0^a\int_0^b\frac{\partial^4 W}{\partial x^4}\sin(\alpha_m x)\sin(\beta_n y)\mathrm{d}x\mathrm{d}y\\&=\alpha_m^4 W_{mn}+\alpha_m^3\int_0^b\left[(-1)^m W\big|_{x=a}-W\big|_{x=0}\right]\sin(\beta_n y)\mathrm{d}y\end{aligned} \tag{4}$$

$$-\alpha_m\int_0^b\left[(-1)^m\left.\frac{\partial^2 W}{\partial x^2}\right|_{x=a}-\left.\frac{\partial^2 W}{\partial x^2}\right|_{x=0}\right]\sin(\beta_n y)\mathrm{d}y$$

$$\begin{aligned}&\int_0^a\int_0^b\frac{\partial^4 W}{\partial y^4}\sin(\alpha_m x)\sin(\beta_n y)\mathrm{d}x\mathrm{d}y\\&=\beta_n^4 W_{mn}+\beta_n^3\int_0^b\left[(-1)^n W\big|_{y=b}-W\big|_{y=0}\right]\sin(\alpha_m x)\mathrm{d}x\\&\quad-\beta_n\int_0^a\left[(-1)^n\left.\frac{\partial^2 W}{\partial y^2}\right|_{y=b}-\left.\frac{\partial^2 W}{\partial y^2}\right|_{y=0}\right]\sin(\alpha_m x)\mathrm{d}x\end{aligned}\tag{5}$$

$$\begin{aligned}&\int_0^a\int_0^b\frac{\partial^4 W}{\partial x^2\partial y^2}\sin(\alpha_m x)\sin(\beta_n y)\mathrm{d}x\mathrm{d}y\\&=\alpha_m^2\beta_n\int_0^a\left[(-1)^n W\big|_{y=b}-W\big|_{y=0}\right]\sin(\alpha_m x)\mathrm{d}x\\&\quad+\alpha_m\beta_n\begin{bmatrix}(-1)^{m+n}W\big|_{\substack{x=a\\y=b}}-(-1)^m W\big|_{\substack{x=a\\y=0}}\\-(-1)^n W\big|_{\substack{x=0\\y=b}}+W\big|_{\substack{x=0\\y=0}}\end{bmatrix}\\&\quad+\alpha_m\beta_n^2\int_0^b\left[(-1)^m W\big|_{x=a}-W\big|_{x=0}\right]\sin(\beta_n y)\mathrm{d}y\\&\quad+\alpha_m^2\beta_n^2 W_{mn}\end{aligned}\tag{6}$$

$$\begin{aligned}&\int_0^a\int_0^b\frac{\partial^2 W}{\partial x^2}\sin(\alpha_m x)\sin(\beta_n y)\mathrm{d}x\mathrm{d}y\\&=-\alpha_m\int_0^b\left[(-1)^m W\big|_{x=a}-W\big|_{x=0}\right]\sin(\beta_n y)\mathrm{d}y-\alpha_m^2 W_{mn}\end{aligned}\tag{7}$$

$$\begin{aligned}&\int_0^a\int_0^b\frac{\partial^2 W}{\partial y^2}\sin(\alpha_m x)\sin(\beta_n y)\mathrm{d}x\mathrm{d}y\\&=-\beta_n\int_0^a\left[(-1)^n W\big|_{y=b}-W\big|_{y=0}\right]\sin(\alpha_m x)\mathrm{d}x-\beta_n^2 W_{mn}\end{aligned}\tag{8}$$

Substituting Eqs. (4)-(8) into Eq. (1) which leads to

$$\begin{aligned}&-\alpha_m\int_0^b\left[(-1)^m\left.\frac{\partial^2 W}{\partial x^2}\right|_{x=a}-\left.\frac{\partial^2 W}{\partial x^2}\right|_{x=0}\right]\sin(\beta_n y)\mathrm{d}y\\&-\beta_n\int_0^a\left[(-1)^n\left.\frac{\partial^2 W}{\partial y^2}\right|_{y=b}-\left.\frac{\partial^2 W}{\partial y^2}\right|_{y=0}\right]\sin(\alpha_m x)\mathrm{d}x\\&+\alpha_m\left[\left(\alpha_m^2+2\beta_n^2\right)-\frac{N_x}{D}\right]\int_0^b\left[(-1)^m W\big|_{x=a}-W\big|_{x=0}\right]\sin(\beta_n y)\mathrm{d}y\\&+\beta_n\left[\left(\beta_n^2+2\alpha_m^2\right)-\frac{N_y}{D}\right]\int_0^a\left[(-1)^n W\big|_{y=b}-W_{y=0}\right]\sin(\alpha_m x)\mathrm{d}x\\&+2\alpha_m\beta_n\left[(-1)^{m+n}W\big|_{\substack{x=a\\y=b}}-(-1)^m W\big|_{\substack{x=a\\y=0}}-(-1)^n W\big|_{\substack{x=0\\y=b}}+W\big|_{\substack{x=0\\y=0}}\right]\\&+\left[\left(\alpha_m^2+\beta_n^2\right)^2-\frac{N_x\alpha_m^2+N_y\beta_n^2}{D}\right]W_{mn}=0\end{aligned}\tag{9}$$

No matter the boundary conditions of the plate are simply supported or clamped, it is well known that $W\big|_{x=0}=W\big|_{x=a}=0$, $W\big|_{y=0}=W\big|_{y=b}=0$, Eq. (9) after further simplification one can get

$$\begin{aligned}&-\alpha_m\int_0^b\left[(-1)^m\left.\frac{\partial^2 W}{\partial x^2}\right|_{x=a}-\left.\frac{\partial^2 W}{\partial x^2}\right|_{x=0}\right]\sin(\beta_n y)\mathrm{d}y\\&-\beta_n\int_0^a\left[(-1)^n\left.\frac{\partial^2 W}{\partial y^2}\right|_{y=b}-\left.\frac{\partial^2 W}{\partial y^2}\right|_{y=0}\right]\sin(\alpha_m x)\mathrm{d}x\\&+\left[\left(\alpha_m^2+\beta_n^2\right)^2-\frac{N_x\alpha_m^2+N_y\beta_n^2}{D}\right]W_{mn}=0\end{aligned}\tag{10}$$

Some parts of Eq. (10) are definite integral, they are the constants. Let

$$\begin{cases}I_m=\int_0^a\left.\frac{\partial^2 W}{\partial y^2}\right|_{y=b}\sin(\alpha_m x)\mathrm{d}x\\J_m=\int_0^a\left.\frac{\partial^2 W}{\partial y^2}\right|_{y=0}\sin(\alpha_m x)\mathrm{d}x\\K_n=\int_0^b\left.\frac{\partial^2 W}{\partial x^2}\right|_{x=a}\sin(\beta_n y)\mathrm{d}y\\L_n=\int_0^b\left.\frac{\partial^2 W}{\partial x^2}\right|_{x=0}\sin(\beta_n y)\mathrm{d}y\end{cases}\tag{11}$$

The unidentified constants I_m, J_m, K_n and L_n have evident physical meaning. When the plate is clamped, or simply supported we can easily obtain

$$\left.\frac{\partial^2 W}{\partial x^2}\right|_{y=0}=\left.\frac{\partial^2 W}{\partial x^2}\right|_{y=b}=0\ ,\ \left.\frac{\partial^2 W}{\partial y^2}\right|_{x=0}=\left.\frac{\partial^2 W}{\partial y^2}\right|_{x=a}=0\tag{12}$$

Substitution of Eq. (12) into I_m, J_m, K_n and L_n leads to

$$\begin{cases}I_m=\int_0^a\left.\left(\frac{\partial^2 W}{\partial y^2}+\mu\frac{\partial^2 W}{\partial x^2}\right)\right|_{y=b}\sin(\alpha_m x)\mathrm{d}x\\J_m=\int_0^a\left.\left(\frac{\partial^2 W}{\partial y^2}+\mu\frac{\partial^2 W}{\partial x^2}\right)\right|_{y=0}\sin(\alpha_m x)\mathrm{d}x\\K_n=\int_0^b\left.\left(\frac{\partial^2 W}{\partial x^2}+\mu\frac{\partial^2 W}{\partial y^2}\right)\right|_{x=a}\sin(\beta_n y)\mathrm{d}y\\L_n=\int_0^b\left.\left(\frac{\partial^2 W}{\partial x^2}+\mu\frac{\partial^2 W}{\partial y^2}\right)\right|_{x=0}\sin(\beta_n y)\mathrm{d}y\end{cases}\tag{13}$$

Obviously, the integrands of $-DI_m$, $-DJ_m$, $-DK_n$ and $-DL_n$ are Fourier coefficients of the bending moments of edges $y=b$, $y=0$, $x=a$ and $x=0$, respectively. The bending moments along the clamped edges can be easily obtained by using the following expressions

$$\begin{cases}M_x\big|_{x=0}=-D\left[\frac{2}{b}\sum_{n=1}^{\infty}L_n\sin(\beta_n y)\right]\\M_x\big|_{x=a}=-D\left[\frac{2}{b}\sum_{n=1}^{\infty}K_n\sin(\beta_n y)\right]\\M_y\big|_{y=0}=-D\left[\frac{2}{a}\sum_{n=1}^{\infty}J_m\sin(\alpha_m x)\right]\\M_y\big|_{y=b}=-D\left[\frac{2}{a}\sum_{n=1}^{\infty}I_m\sin(\alpha_m x)\right]\end{cases}\tag{14}$$

For simply supported plate, the corresponding unknowns will be zero. Accordingly Eq. (10) is expressed by an unidentified constants I_m, J_m, K_n and L_n as

$$W_{mn}=\frac{\beta_n\left[(-1)^n I_m-J_m\right]+\alpha_m\left[(-1)^m K_n-L_n\right]}{\left(\alpha_m^2+\beta_n^2\right)^2-\dfrac{N_x\alpha_m^2+N_y\beta_n^2}{D}} \tag{15}$$

By substitution of Eq. (15) into Eq. (3), the expression for $W(x,y)$ is obtained as follow, here $m=1,2,3,\cdots$ and n=1,2,3,…

$$\begin{aligned}&W(x,y)\\&=\frac{4}{ab}\sum_{m=1}^{\infty}\sum_{n=1}^{\infty}\frac{\beta_n\left[(-1)^n I_m-J_m\right]+\alpha_m\left[(-1)^m K_n-L_n\right]}{\left(\alpha_m^2+\beta_n^2\right)^2-\dfrac{N_x\alpha_m^2+N_y\beta_n^2}{D}}\\&\times\sin(\alpha_m x)\sin(\beta_n y)\end{aligned} \tag{16}$$

A class of complex three (BVPs) are studied, i.e. plate with all four edges clamped (CCCC), plate with three clamped edges and one simply supported edge (CCCS), and plate with two adjacent edges clamped and the other simply supported (CCSS), where C denotes the clamped and S denotes the simply supported edge. Here we consider the uniaxial uniform in-plane loads acted at the two opposite edges, thus a CCCS plate can be loaded in two ways, one with the two opposite edges clamped and the other with one clamped and other simply supported edge. Thus, total of four cases of boundary conditions are studied which are presented below.

Case 1

When the rectangular plate is fully clamped, uniform uniaxial in-plane loads are applied along the x direction at edge x=0 and x=a. Eq. (16) satisfy the boundary conditions of $W\big|_{x=0}=W\big|_{x=a}=0$, $W\big|_{y=0}=W\big|_{y=b}=0$, and it has necessary to satisfy the boundary conditions of $\left.\frac{\partial W}{\partial x}\right|_{x=0}=\left.\frac{\partial W}{\partial x}\right|_{x=a}=0$, $\left.\frac{\partial W}{\partial y}\right|_{y=0}=\left.\frac{\partial W}{\partial y}\right|_{y=b}=0$, then one can obtain

$$\frac{4}{ab}\sum_{n=1}^{\infty}\sum_{m=1}^{\infty}\alpha_m W_{mn}\sin(\beta_n y)=0 \tag{17}$$

$$\frac{4}{ab}\sum_{n=1}^{\infty}\sum_{m=1}^{\infty}(-1)^m\alpha_m W_{mn}\sin(\beta_n y)=0 \tag{18}$$

$$\frac{4}{ab}\sum_{m=1}^{\infty}\sum_{n=1}^{\infty}\beta_n W_{mn}\sin(\alpha_m x)=0 \tag{19}$$

$$\frac{4}{ab}\sum_{m=1}^{\infty}\sum_{n=1}^{\infty}(-1)^n\beta_n W_{mn}\sin(\alpha_m x)=0 \tag{20}$$

Multiplying Eqs. (17) and (18) by $\sin(\beta_n y)\mathrm{d}y$ then through integration from 0 to b produces Eqs. (21) and (22). Multiplying Eqs. (19) and (20) by $\sin(\alpha_m x)\mathrm{d}x$ then through integration from 0 to a yields Eqs. (23) and (24) and can be expressed as

$$\begin{aligned}&\sum_{m=1}^{\infty}\frac{\alpha_m}{\left(\alpha_m^2+\beta_n^2\right)^2-\dfrac{N_x\alpha_m^2}{D}}\\&\times\left\{\beta_n\left[(-1)^n I_m-J_m\right]+\alpha_m\left[(-1)^m K_n-L_n\right]\right\}=0\end{aligned} \tag{21}$$

for n=1, 2, 3, …,

$$\begin{aligned}&\sum_{m=1}^{\infty}\frac{(-1)^m\alpha_m}{\left(\alpha_m^2+\beta_n^2\right)^2-\dfrac{N_x\alpha_m^2}{D}}\\&\times\left\{\beta_n\left[(-1)^n I_m-J_m\right]+\alpha_m\left[(-1)^m K_n-L_n\right]\right\}=0\end{aligned} \tag{22}$$

for n=1, 2, 3, …,

$$\begin{aligned}&\sum_{n=1}^{\infty}\frac{\beta_n}{\left(\alpha_m^2+\beta_n^2\right)^2-\dfrac{N_x\alpha_m^2}{D}}\\&\times\left\{\beta_n\left[(-1)^n I_m-J_m\right]+\alpha_m\left[(-1)^m K_n-L_n\right]\right\}=0\end{aligned} \tag{23}$$

for m=1, 2, 3, …, and

$$\begin{aligned}&\sum_{n=1}^{\infty}\frac{(-1)^n\beta_n}{\left(\alpha_m^2+\beta_n^2\right)^2-\dfrac{N_x\alpha_m^2}{D}}\\&\times\left\{\beta_n\left[(-1)^n I_m-J_m\right]+\alpha_m\left[(-1)^m K_n-L_n\right]\right\}=0\end{aligned} \tag{24}$$

for m=1, 2, 3, …,

Eqs. (21)-(24) are sets of four linear algebraic simultaneous equations in terms of I_m, J_m, K_n and L_n. The buckling load factor is achieved by taking the determinant of the matrix equal to zero. By Mathematica software the "Findroot" command is used to search for the numerical roots of the buckling load equation. Although an exact solution of the buckling load factors is observed from the derivation when m, $n \to \infty$, practically a convergence solutions with desired accuracy is obtained by taking few number of terms ($m,n=20$), which is the primary advantage of the present method. Putting the critical buckling load into the coefficient matrix of the Eqs. (21)-(24) to obtain I_m, J_m, K_n and L_n. Then, the associated buckling mode shapes are obtained from the inversion formula using Wolfram Mathematica11.3 software.

Case 2

When the rectangular plate clamped at edges x=0,a and y=0, simply supported at edge y=b,, and is exposed to uniform in-plane loads along the x direction. The deflection of the plate can be expressed as follow

$$W(x,y) \tag{25}$$

$$= \frac{4}{ab}\sum_{m=1}^{\infty}\sum_{n=1}^{\infty}\frac{-\beta_n J_m + \alpha_m\left[(-1)^m K_n - L_n\right]}{\left(\alpha_m^2+\beta_n^2\right)^2 - \frac{N_x\alpha_m^2}{D}} \times \sin(\alpha_m x)\sin(\beta_n y)$$

Eq. (25) satisfy the boundary conditions of $\left.\frac{\partial W}{\partial x}\right|_{x=0} = \left.\frac{\partial W}{\partial x}\right|_{x=a} = 0$, $\left.\frac{\partial W}{\partial y}\right|_{y=0} = 0$, then one can obtain

$$\sum_{m=1}^{\infty}\frac{\alpha_m}{\left(\alpha_m^2+\beta_n^2\right)^2 - \frac{N_x\alpha_m^2}{D}} \times\left\{-\beta_n J_m + \alpha_m\left[(-1)^m K_n - L_n\right]\right\} = 0 \quad n=1,2,3,\cdots \tag{26}$$

$$\sum_{m=1}^{\infty}\frac{(-1)^m\alpha_m}{\left(\alpha_m^2+\beta_n^2\right)^2 - \frac{N_x\alpha_m^2}{D}} \times\left\{-\beta_n J_m + \alpha_m\left[(-1)^m K_n - L_n\right]\right\} = 0 \quad n=1,2,3,\cdots \tag{27}$$

$$\sum_{n=1}^{\infty}\frac{\beta_n}{\left(\alpha_m^2+\beta_n^2\right)^2 - \frac{N_x\alpha_m^2}{D}} \times\left\{-\beta_n J_m + \alpha_m\left[(-1)^m K_n - L_n\right]\right\} = 0 \quad m=1,2,3,\cdots \tag{28}$$

Eqs. (26)-(28) are sets of three linear algebraic simultaneous equations in terms of J_m, K_n and L_n. The buckling load factor is achieved by taking the determinant of the matrix equal to zero. Although an exact solution of the buckling load factors is observed from the derivation when m, $n \to \infty$, practically a convergence solutions with desired accuracy is obtained by taking few number of terms ($m, n = 20$), which is the primary advantage of the present method. Putting the critical buckling load into the coefficient matrix of the Eqs. (26)-(28) to obtain J_m, K_n and L_n. Then, the associated buckling mode shapes are obtained from the inversion formula using Wolfram Mathematica11.3 software.

Case 3

When the rectangular plate is clamped at edges x=0 and y=0, b, simply supported at edge x=a, and a plate under uniform uniaxial in-plane load along the x direction. The deflection of the plate can be expressed as follow

$$W(x,y) = \frac{4}{ab}\sum_{m=1}^{\infty}\sum_{n=1}^{\infty}\frac{\beta_n\left[(-1)^n I_m - J_m\right] - \alpha_m L_n}{\left(\alpha_m^2+\beta_n^2\right)^2 - \frac{N_x\alpha_m^2}{D}} \times\sin(\alpha_m x)\sin(\beta_n y) \tag{29}$$

Eq. (29) still needs to satisfy the boundary conditions of $\left.\frac{\partial W}{\partial x}\right|_{x=0} = 0$, $\left.\frac{\partial W}{\partial y}\right|_{y=0} = \left.\frac{\partial W}{\partial y}\right|_{y=b} = 0$, then one can get

$$\sum_{m=1}^{\infty}\frac{\alpha_m}{\left(\alpha_m^2+\beta_n^2\right)^2 - \frac{N_x\alpha_m^2}{D}} \times\left\{\beta_n\left[(-1)^n I_m - J_m\right] - \alpha_m L_n\right\} = 0 \quad n=1,2,3,\cdots \tag{30}$$

$$\sum_{n=1}^{\infty}\frac{\beta_n}{\left(\alpha_m^2+\beta_n^2\right)^2 - \frac{N_x\alpha_m^2}{D}} \times\left\{\beta_n\left[(-1)^n I_m - J_m\right] - \alpha_m L_n\right\} = 0 \quad m=1,2,3,\cdots \tag{31}$$

$$\sum_{n=1}^{\infty}\frac{(-1)^n\beta_n}{\left(\alpha_m^2+\beta_n^2\right)^2 - \frac{N_x\alpha_m^2}{D}} \times\left\{\beta_n\left[(-1)^n I_m - J_m\right] - \alpha_m L_n\right\} = 0 \quad m=1,2,3,\cdots \tag{32}$$

Eqs. (30)-(32) are sets of three linear algebraic simultaneous equations in terms of I_m, J_m and L_n. The buckling load factor is achieved by taking the determinant of the matrix equal to zero. A convergence solutions with desired accuracy is obtained by taking few number of terms ($m, n = 20$), which is the main advantage of the present method. Putting the critical buckling load into the coefficient matrix of the Eqs. (30)-(32) to obtain I_m, J_m and L_n. Then, the associated buckling mode shapes are obtained from the inversion formula using Wolfram Mathematica11.3 software.

Case 4

When the rectangular plate is clamped at edges x=0 and y=0, simply supported at edge x=a and y=b, a uniaxial uniform in-plane load is applied in the x direction. The deflection of the plate reduce to

$$W(x,y) = \frac{4}{ab}\sum_{m=1}^{\infty}\sum_{n=1}^{\infty}\frac{-\left(\beta_n J_m + \alpha_m L_n\right)}{\left(\alpha_m^2+\beta_n^2\right)^2 - \frac{N_x\alpha_m^2}{D}}\sin(\alpha_m x)\sin(\beta_n y) \tag{33}$$

Eq. (33) has to satisfy the boundary conditions of $\left.\frac{\partial W}{\partial x}\right|_{x=0} = 0$ and $\left.\frac{\partial W}{\partial y}\right|_{y=0} = 0$, then one can obtain

$$\sum_{m=1}^{\infty}\frac{\alpha_m}{\left(\alpha_m^2+\beta_n^2\right)^2 - \frac{N_x\alpha_m^2}{D}}\left(-\beta_n J_m - \alpha_m L_n\right) = 0 \tag{34}$$

for n=1, 2, 3, …,

$$\sum_{n=1}^{\infty}\frac{\beta_n}{\left(\alpha_m^2+\beta_n^2\right)^2 - \frac{N_x\alpha_m^2}{D}}\left(-\beta_n J_m - \alpha_m L_n\right) = 0 \tag{35}$$

for m=1, 2, 3, …,

Eqs. (34) and (35) are sets of two linear algebraic simultaneous equations in terms of J_m and L_n. Same solution procedure is adopted for Case 4.

Table 1 First ten buckling load factors, $N_x a^2/(D\pi^2)$, of the CCCC rectangular plates

b/a	Method	Mode									
		1st	2nd	3rd	4th	5th	6th	7th	8th	9th	10th
	Present	31.468	32.348	41.123	46.201	60.818	69.886	90.330	90.692	91.213	92.178
0.5	FEM	31.476	32.355	41.144	46.244	60.916	70.008	90.368	90.720	91.480	92.320
	Wang *et al.* (2016)	31.468	32.348	41.123	46.201	60.818	69.886	90.330	90.692	91.213	92.178
	Present	10.074	11.610	19.465	24.891	26.373	26.833	36.089	38.712	40.651	47.704
1	FEM	10.075	11.611	19.470	24.894	26.378	26.844	36.101	38.736	40.666	47.716
	Wang *et al.* (2016)	10.074	11.610	19.465	24.891	26.373	26.833	36.089	38.712	40.651	47.704
	Present	5.8251	9.4230	13.319	13.574	17.198	21.812	22.797	24.814	25.256	28.617
1.5	FEM	5.8253	9.4240	13.321	13.576	17.201	21.815	22.802	24.819	25.263	28.620
	Wang *et al.* (2016)	5.8251	9.4230	13.319	13.574	17.198	21.812	22.797	24.814	25.256	28.617
	Present	4.8347	8.0673	8.8175	10.908	14.990	15.124	16.650	18.668	21.855	23.256
2	FEM	4.8350	8.0675	8.8183	10.908	14.992	15.126	16.653	18.671	21.859	23.260
	Wang *et al.* (2016)	4.8347	8.0673	8.8575	10.908	14.990	15.124	16.650	18.668	21.855	23.256
	Present	4.4740	6.1935	8.5680	9.7970	9.9347	12.088	15.786	16.253	16.379	17.639
2.5	FEM	4.4742	6.1938	8.5688	9.7970	9.9363	12.089	15.789	16.257	16.382	17.642
	Wang *et al.* (2016)	4.4740	6.1935	8.5680	9.7979	9.9347	12.088	15.786	16.253	16.379	17.639
	Present	4.3050	5.3609	7.5597	8.4415	9.2515	10.717	11.418	13.005	16.246	16.339
3	FEM	4.3052	5.3611	7.5608	8.4420	9.2525	10.718	11.421	13.007	16.248	16.342
	Wang *et al.* (2016)	4.3050	5.3609	7.5597	8.4415	9.2515	10.717	11.418	13.005	16.246	16.339
	Present	4.2127	4.9253	6.3509	8.3684	8.8054	8.9432	9.9624	11.516	12.596	13.728
3.5	FEM	4.2129	4.9256	6.3514	8.3690	8.8065	8.9437	9.9633	11.518	12.599	13.731
	Wang *et al.* (2016)	4.2127	4.9253	6.3509	8.3684	8.8054	8.9432	9.9624	11.516	12.596	13.728
	Present	4.1568	4.6701	5.6643	7.3323	8.3225	8.7519	9.5029	9.9028	10.628	12.200
4	FEM	4.1571	4.6705	5.6649	7.3338	8.3238	8.7531	9.5044	9.9075	10.631	12.203
	Wang *et al.* (2016)	4.1568	4.6701	5.6643	7.3323	8.3225	8.7519	9.5029	9.9028	10.628	12.200
	Present	4.1205	4.5080	5.2398	6.4281	8.2584	8.2918	8.6249	9.2019	10.055	10.858
4.5	FEM	4.1206	4.5082	5.2400	6.4390	8.2602	8.2928	8.6257	9.2025	10.056	10.862
	Wang *et al.* (2016)	4.1205	4.5080	5.2398	6.4381	8.2584	8.2918	8.6249	9.2019	10.055	10.858
	Present	4.0954	4.3986	4.9598	5.8595	7.2037	8.2702	8.5362	8.9938	9.1117	9.6642
5	FEM	4.0956	4.3988	4.9600	5.8600	7.2052	8.2712	8.5372	8.9948	9.1148	9.6652
	Wang *et al.* (2016)	4.0954	4.3986	4.9598	5.8595	7.2037	8.2702	8.5362	8.9938	9.1117	9.6642

3. Numerical and graphical results

Using the method described in Section 2, the buckling solutions of rectangular thin plates are found for different boundary conditions and aspect ratios. The results are presented for aspect ratio's 0.5, 1, 1.5, 2, 2.5, 3, 3.5, 4, 4.5, and 5 respectively. To verify the correctness of the present method, the results are compared with the FEA using (ABAQUS) software Simulia (2013), with thickness to width ratio 10^{-4}, and convergence is achieved using 4-node thin shell element S4R and uniform mesh size with short edge length of $1/400$. Four complex BVPs of the plate with different aspect ratios are studied. Table 1 shows the buckling factor denoted by $N_x a^2/(D\pi^2)$ of rectangular thin plates under CCCC boundary condition with aspect ratios being 0.5, 1, 1.5, 2, 2.5, 3, 3.5, 4, 4.5, and 5. Fig. 2 shows the comparison of first ten mode shapes obtained by present method using Mathematica software and the FEA using (ABAQUS) software. The present results are validated by extensive numerical comparison with the FEA using (ABAQUS) software and the existing analytical solutions and show satisfactory agreement.

Tables 2-4 present the buckling load factors for CCCS, CCSS rectangular thin plates subjected to uniaxial uniform in-plane compression load. The present results are very close to the numerical solutions obtained by commercial software (ABAQUS), and the existing analytical solution which verify the accuracy of the method. Figs. 3-5 show the buckling mode shapes comparison of the present method and the FEA which shows satisfactory agreement. Tables 1-4 and Figs. 2-5 show that the present method is consistent with the finite element method and the existing literature, which verifies the accuracy and effectiveness of the method.

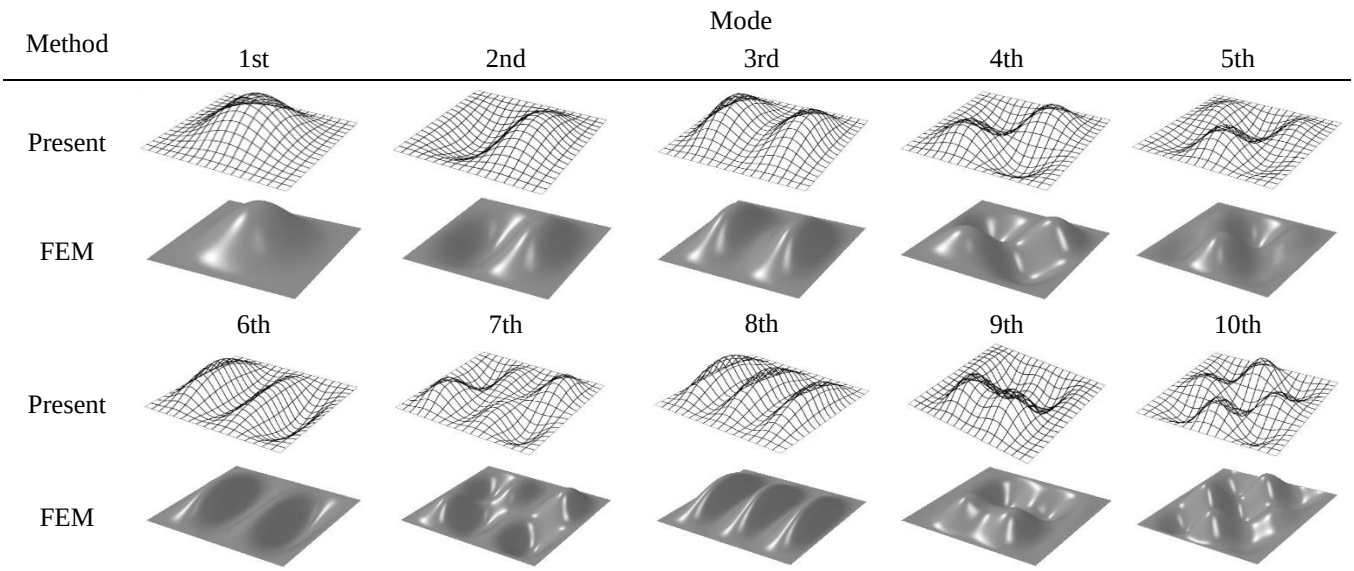

Fig. 2 First ten buckling mode shapes of CCCC square thin plate

Table 2 First ten buckling load factors of the CCCS rectangular plates loaded at two opposite clamped edges

b/*a*	Method	Mode									
		1st	2nd	3rd	4th	5th	6th	7th	8th	9th	10th
0.5	Present	24.891	26.373	36.089	40.651	53.945	58.384	75.776	78.470	79.504	89.657
	FEM	24.892	26.376	36.095	40.660	53.960	58.408	75.820	78.488	79.520	89.724
	Wang *et al.* (2016)	24.891	26.373	36.089	40.651	53.945	58.384	75.776	78.470	79.504	89.657
1	Present	8.0673	10.908	18.668	21.855	24.005	26.524	34.535	34.833	38.437	43.448
	FEM	8.0675	10.909	18.672	21.856	24.008	26.532	34.544	34.840	38.454	43.455
	Wang *et al.* (2016)	8.0673	10.908	18.668	21.855	24.005	26.524	34.535	34.833	38.437	43.448
1.5	Present	5.3609	9.2515	11.418	13.005	17.054	20.819	20.973	23.164	25.164	28.273
	FEM	5.3613	9.2542	11.420	13.008	17.064	20.829	20.976	23.169	25.189	28.297
	Wang *et al.* (2016)	5.3609	9.2515	11.418	13.005	17.054	20.819	20.973	23.164	25.164	28.273
2	Present	4.6701	7.3323	8.7519	10.628	13.540	14.308	16.565	18.420	20.555	22.124
	FEM	4.6708	7.3333	8.7548	10.631	13.543	14.312	16.575	18.431	20.561	22.134
	Wang *et al.* (2016)	4.6701	7.3323	8.7519	10.628	13.540	14.308	16.565	18.420	20.555	22.124
2.5	Present	4.3986	5.8595	8.5362	9.1117	9.6642	11.769	14.942	15.178	16.353	17.470
	FEM	4.3989	5.8598	8.5370	9.1133	9.6651	11.771	14.947	15.182	16.355	17.474
	Wang *et al.* (2016)	4.3986	5.8595	8.5362	9.1117	9.6642	11.769	14.942	15.178	16.353	17.470
3	Present	4.2646	5.1845	7.1210	8.4237	9.1783	10.544	10.592	12.679	15.797	15.915
	FEM	4.2656	5.1854	7.1223	8.4279	9.1824	10.548	10.595	12.683	15.802	15.920
	Wang *et al.* (2016)	4.2646	5.1845	7.1210	8.4237	9.1783	10.544	10.592	12.679	15.797	15.915
3.5	Present	4.1886	4.8216	6.0949	8.3113	8.3576	8.8986	9.8581	11.322	11.803	13.407
	FEM	4.1892	4.8222	6.0957	8.3127	8.3608	8.9012	9.8612	11.325	11.805	13.410
	Wang *et al.* (2016)	4.1886	4.8216	6.0949	8.3113	8.3576	8.8986	9.8581	11.322	11.803	13.407
4	Present	4.1413	4.6042	5.5033	7.0212	8.3154	8.7227	9.3851	9.4352	10.503	11.995
	FEM	4.1423	4.6051	5.5043	7.0225	8.3194	8.7269	9.3869	9.4394	10.508	11.999
	Wang *et al.* (2016)	4.1413	4.6042	5.5033	7.0212	8.3154	8.7227	9.3851	9.4352	10.503	11.995
4.5	Present	4.1099	4.4635	5.1323	6.2316	7.9118	8.2869	8.6048	9.1555	9.9702	10.336
	FEM	4.1108	4.4645	5.1323	6.2326	7.9131	8.2909	8.6089	9.1595	9.9743	10.338
	Wang *et al.* (2016)	4.1099	4.4635	5.1333	6.2316	7.9118	8.2869	8.6048	9.1555	9.9702	10.336
5	Present	4.0879	4.3672	4.8846	5.7160	6.9630	8.2667	8.5218	8.7444	8.9606	9.6036
	FEM	4.0888	4.3680	4.8856	5.7168	6.9644	8.2708	8.5260	8.7460	8.9648	9.6076
	Wang *et al.* (2016)	4.0879	4.3672	4.8846	5.7160	6.9630	8.2667	8.5218	8.7444	8.9606	9.6036

Table 3 First ten buckling load factors of the CCCS rectangular plates loaded at simply supported edge and its opposite clamped edge

b/*a*	Method	Mode									
		1st	2nd	3rd	4th	5th	6th	7th	8th	9th	10th
0.5	Present	28.832	32.234	36.116	42.914	53.313	66.104	80.336	87.521	90.672	92.152
	FEM	28.835	32.242	36.127	42.948	53.380	66.220	80.508	87.548	90.704	92.300
	Wang *et al.* (2016)	28.832	32.234	36.116	42.914	53.313	66.104	80.336	87.521	90.672	92.152
1	Present	8.0870	10.281	15.205	22.673	22.803	25.187	30.891	32.602	39.225	44.477
	FEM	8.0874	10.281	15.207	22.676	22.811	25.191	30.898	32.602	39.239	44.509
	Wang *et al.* (2016)	8.0870	10.281	15.205	22.673	22.803	25.187	30.891	32.619	39.225	44.477
1.5	Present	3.9331	7.3748	10.811	13.200	13.318	17.390	20.598	21.124	23.533	24.681
	FEM	3.9332	7.3756	10.812	13.201	13.319	17.392	20.601	21.128	23.536	24.685
	Wang *et al.* (2016)	3.9331	7.3748	10.811	13.200	13.318	17.390	20.598	21.124	23.533	24.681
2	Present	2.9025	6.2226	6.7082	9.0222	12.232	12.644	14.596	15.151	18.774	19.618
	FEM	2.9025	6.2230	6.7088	9.0230	12.234	12.645	14.598	15.153	18.777	19.622
	Wang *et al.* (2016)	2.9025	6.2226	6.7082	9.0222	12.232	12.644	14.596	15.151	18.774	19.618
2.5	Present	2.5294	4.3002	6.4420	7.7470	8.0683	10.436	12.419	13.114	13.570	15.718
	FEM	2.5294	4.3006	6.4427	7.7477	8.0702	10.434	12.421	13.118	13.572	15.721
	Wang *et al.* (2016)	2.5294	4.3002	6.4420	7.7470	8.0683	10.436	12.419	13.114	13.570	15.718
3	Present	2.3558	3.4386	5.6993	6.3141	7.1541	8.7531	9.4458	11.639	12.297	13.077
	FEM	2.3558	3.4387	5.6998	6.3143	7.1547	8.7540	9.4478	11.641	12.299	13.079
	Wang *et al.* (2016)	2.3558	3.4386	5.6993	6.3141	7.1541	8.7531	9.4458	11.639	12.297	13.077
3.5	Present	2.2613	2.9891	4.4566	6.2363	6.8075	6.9854	7.9095	9.6653	10.462	12.225
	FEM	2.2614	2.9892	4.4571	6.2369	6.8078	6.9865	7.9095	9.6661	10.465	12.227
	Wang *et al.* (2016)	2.2613	2.9891	4.4566	6.2363	6.8075	6.9854	7.9099	9.6653	10.462	12.225
4	Present	2.2044	2.7269	3.7476	5.4637	6.1887	6.6310	7.4083	8.0548	8.6338	10.487
	FEM	2.2044	2.7271	3.7481	5.4653	6.1894	6.6319	7.4094	8.0594	8.6356	10.491
	Wang *et al.* (2016)	2.2044	2.7269	3.7476	5.4637	6.1887	6.6310	7.4083	8.0548	8.6338	10.487
4.5	Present	2.1674	2.5609	3.3099	4.5434	6.1562	6.4069	6.4979	7.1004	7.9983	8.9637
	FEM	2.1675	2.5610	3.3102	4.5441	6.1565	6.4084	6.4983	7.1012	7.9990	8.9674
	Wang *et al.* (2016)	2.1674	2.5609	3.3099	4.5434	6.1562	6.4069	6.4979	7.1004	7.9983	8.9637
5	Present	2.1420	2.4493	3.0220	3.9464	5.3296	6.1354	6.4057	6.8788	7.2588	7.5935
	FEM	2.1421	2.4494	3.0220	3.9470	5.3308	6.1356	6.4064	6.8792	7.2616	7.5944
	Wang *et al.* (2016)	2.1420	2.4493	3.0220	3.9464	5.3296	6.1354	6.4057	6.8792	7.2588	7.5935

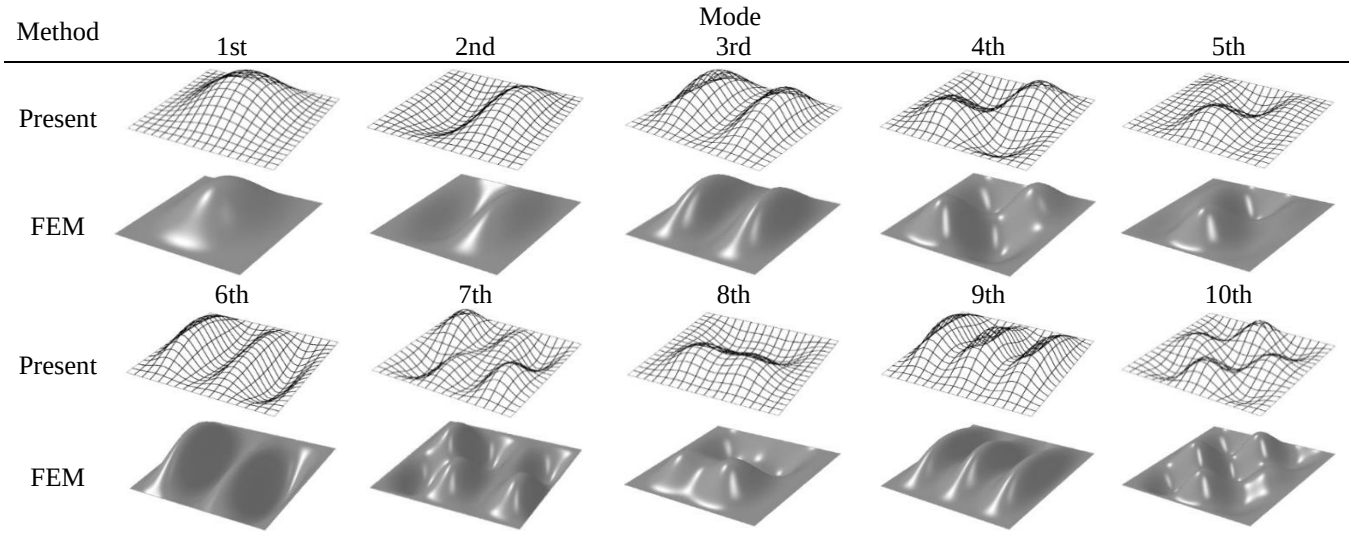

Fig. 3 First ten buckling mode shapes of CCCS square plate loaded at two opposite clamped edges

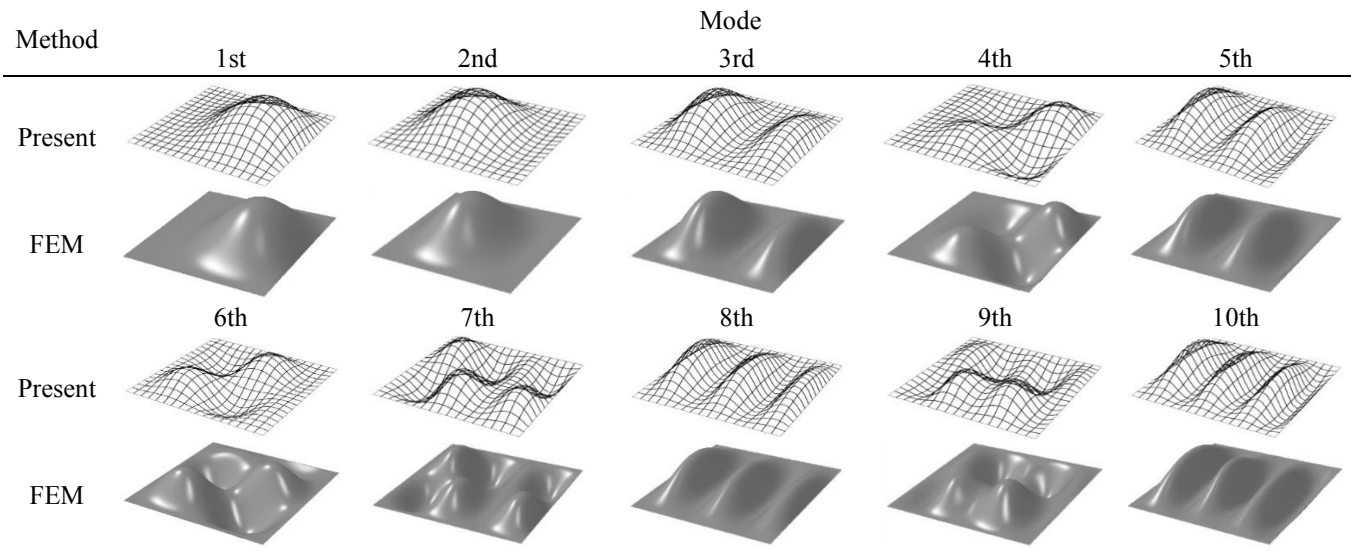

Fig. 4 First ten buckling mode shapes of CCCS square thin plate loaded at clamped edge with opposite simply supported edge

Table 4 First ten buckling load factors of the CCSS rectangular plates

b/*a*	Method	Mode									
		1st	2nd	3rd	4th	5th	6th	7th	8th	9th	10th
0.5	Present	22.673	25.187	30.891	39.225	47.525	54.515	66.528	75.982	78.758	81.849
	FEM	22.674	25.189	30.895	39.233	47.536	54.532	66.560	75.996	78.776	81.904
	Wang *et al.* (2016)	22.673	25.187	30.891	39.225	47.525	54.515	66.528	75.982	78.758	81.849
1	Present	6.2226	9.0222	14.596	19.618	22.414	22.803	28.879	32.295	34.931	40.982
	FEM	6.2228	9.0228	14.598	19.619	22.420	22.805	28.884	32.309	34.939	40.988
	Wang *et al.* (2016)	6.2226	9.0222	14.596	19.618	22.414	22.803	28.879	32.295	34.931	40.982
1.5	Present	3.4386	7.1541	9.4458	11.639	13.077	16.606	18.680	21.032	22.105	24.220
	FEM	3.4387	7.1551	9.4462	11.640	13.080	16.608	18.682	21.040	22.108	24.228
	Wang *et al.* (2016)	3.4386	7.1541	9.4458	11.639	13.077	16.606	18.680	21.032	22.105	24.220
2	Present	2.7269	5.4637	6.6310	8.6338	11.228	12.597	13.558	14.396	17.919	18.231
	FEM	2.7270	5.4640	6.6320	8.6350	11.229	12.601	13.560	14.400	17.923	18.233
	Wang *et al.* (2016)	2.7269	5.4637	6.6310	8.6338	11.228	12.597	13.558	14.396	17.919	18.231
2.5	Present	2.4493	3.9464	6.4057	7.2588	7.5935	9.9329	12.304	12.393	13.473	14.925
	FEM	2.4494	3.9467	6.4072	7.2594	7.5950	9.9347	12.306	12.399	13.479	14.928
	Wang *et al.* (2016)	2.4493	3.9464	6.4057	7.2588	7.5935	9.9329	12.304	12.393	13.473	14.925
3	Present	2.3129	3.2512	5.2433	6.2911	7.0683	8.5055	8.7375	11.052	12.284	13.012
	FEM	2.3131	3.2514	5.2437	6.2929	7.0701	8.5073	8.7387	11.054	12.291	13.018
	Wang *et al.* (2016)	2.3129	3.2512	5.2433	6.2911	7.0683	8.5055	8.7375	11.052	12.284	13.012
3.5	Present	2.2358	2.8791	4.1863	6.2226	6.4579	6.7794	7.7837	9.3823	9.8419	12.029
	FEM	2.2360	2.8793	4.1865	6.2242	6.4584	6.7810	7.7852	9.3837	9.8433	12.031
	Wang *et al.* (2016)	2.2358	2.8791	4.1863	6.2226	6.4579	6.7794	7.7837	9.3823	9.8419	12.029
4	Present	2.1880	2.6570	3.5770	5.1388	6.1805	6.5952	7.3292	7.5446	8.4778	10.167
	FEM	2.1883	2.6574	3.5774	5.1394	6.1835	6.5981	7.3325	7.5463	8.4813	10.171
	Wang *et al.* (2016)	2.1880	2.6570	3.5770	5.1388	6.1805	6.5952	7.3292	7.5446	8.4778	10.167
4.5	Present	2.1562	2.5139	3.1960	4.3255	6.0501	6.1522	6.4749	7.0417	7.8971	8.4726
	FEM	2.1562	2.5141	3.1963	4.3259	6.0509	6.1546	6.4770	7.0440	7.8993	8.4736
	Wang *et al.* (2016)	2.1562	2.5139	3.1960	4.3255	6.0501	6.1522	6.4749	7.0417	7.8971	8.4726
5	Present	2.1341	2.4161	2.6423	3.7946	5.0784	6.1311	6.3893	6.8329	6.9030	7.5103
	FEM	2.1343	2.4163	2.6426	3.7949	5.0779	6.1332	6.3916	6.8348	6.9040	7.5124
	Wang *et al.* (2016)	2.1341	2.4161	2.6423	3.7946	5.0784	6.1311	6.3893	6.8329	6.9030	7.5103

Table 5 Convergence study for CCCC plates, with b/a=0.5 and 4.5

b/a	No of series terms	Mode									
		1st	2nd	3rd	4th	5th	6th	7th	8th	9th	10th
0.5	10	31.468	32.348	41.122	46.195	60.812	69.863	90.319	90.691	91.180	92.174
	15	31.468	32.348	41.123	46.201	60.817	69.885	90.330	90.692	91.211	92.178
	20	**31.468**	**32.348**	**41.123**	**46.201**	**60.818**	**69.885**	**90.330**	**90.692**	**91.213**	**92.178**
	30	31.468	32.348	41.123	46.201	60.818	69.885	90.330	90.692	91.213	92.178
4.5	10	4.1203	4.5076	5.2382	6.4361	8.2529	8.2916	8.6241	9.1991	10.051	10.854
	15	4.1204	4.5080	5.2397	6.4378	8.2580	8.2918	8.6246	9.2015	10.054	10.858
	20	**4.1204**	**4.5080**	**5.2398**	**6.4381**	**8.2584**	**8.2918**	**8.6249**	**9.2019**	**10.055**	**10.858**
	30	4.1204	4.5080	5.2398	6.4381	8.2584	8.2918	8.6249	9.2019	10.055	10.858

Table 6 Convergence study for CCCS plates loaded at two opposite clamped edges, with b/a=0.5 and 4.5

b/a	No of series terms	Mode									
		1st	2nd	3rd	4th	5th	6th	7th	8th	9th	10th
0.5	10	24.891	26.373	36.089	40.650	53.945	58.381	75.764	78.470	79.500	89.644
	15	24.891	26.373	36.089	40.651	53.945	58.384	75.776	78.470	79.504	89.656
	20	**24.981**	**26.373**	**36.089**	**40.651**	**53.945**	**58.384**	**75.776**	**78.470**	**79.504**	**89.657**
	30	24.981	26.373	36.089	40.651	53.945	58.384	75.776	78.470	79.504	89.657
4.5	10	4.1098	4.4633	5.1317	6.2304	7.9098	8.2868	8.6043	9.1544	9.9680	10.333
	15	4.1099	4.4635	5.1323	6.2314	7.9116	8.2869	8.6047	9.1553	9.9698	10.336
	20	**4.1099**	**4.4635**	**5.1323**	**6.2315**	**7.9118**	**8.2869**	**8.6048**	**9.1555**	**9.9702**	**10.336**
	30	4.1099	4.4635	5.1323	6.2315	7.9118	8.2869	8.6048	9.1555	9.9702	10.336

Table 7 Convergence study for CCCS plates loaded at simply supported edge and its opposite clamped edges, with b/a=0.5 and 4.5

b/a	No of series terms	Mode									
		1st	2nd	3rd	4th	5th	6th	7th	8th	9th	10th
0.5	10	28.831	32.233	36.116	42.913	53.310	66.096	80.320	87.520	90.685	92.149
	15	28.832	32.234	36.116	42.914	53.313	66.104	80.335	87.521	90.673	92.152
	20	**28.832**	**32.234**	**36.116**	**42.914**	**53.313**	**66.104**	**80.336**	**87.521**	**90.672**	**92.152**
	30	28.832	32.234	36.116	42.914	53.313	66.104	80.336	87.521	90.672	92.152
4.5	10	2.1674	2.5608	3.3095	4.5431	6.1561	6.4063	6.4976	7.0991	7.9968	8.9636
	15	2.1674	2.5609	3.3099	4.5434	6.1562	6.4069	6.4978	7.1003	7.9979	8.9647
	20	**2.1674**	**2.5609**	**3.3099**	**4.5434**	**6.1562**	**6.4069**	**6.4979**	**7.1004**	**7.9983**	**8.9637**
	30	2.1674	2.5609	3.3099	4.5434	6.1562	6.4069	6.4979	7.1004	7.9983	8.9637

Tables 1-4 show that when the aspect ratio increases the buckling load factor is decreases vice versa. Consequently, the buckling load factor has the minimum value at aspect ratio (0.5) for all boundary conditions. It is also observed that when the aspect ratio is 1 or less, the buckling load coefficient decreases rapidly. However, when the aspect ratio increases from 1 to 5, very small changes are observed. Therefore, it can be stated that the aspect ratio has a great influence on the buckling load coefficient. From Tables 1-4, it can be seen that the buckling load factor of plate with aspect ratios 0.5 are about 3, 5.5 and 6.5 times higher than plates with aspect ratios of 1, 1.5 and 2, respectively.

It can also be seen that the boundary conditions also affect the buckling loads. When the aspect ratio is less than 1, the buckling loads under all boundary conditions are higher. The buckling load factor of CCCC is always greater than that of CCCS and CCSS for all aspect ratios.

In addition, the buckling load coefficient of CCCS is always higher than that of CCSS. The results show that the clamped edges can improve the mechanical buckling strength of the plate more efficiently than the simply supported edges.

Tables 5-8 present the convergence results of all four types of boundary conditions. The result shows that the convergence is very fast. The high accuracy of five significant figures is attained by taking only 20 numbers of terms in our solution.

Table 8 Convergence study for the CCSS plates, with b/a=0.5 and 4.5

b/*a*	No of series terms	Mode									
		1st	2nd	3rd	4th	5th	6th	7th	8th	9th	10th
0.5	10	22.673	25.187	30.891	39.224	47.524	54.514	66.525	75.982	78.757	81.841
	15	22.673	25.187	30.891	39.225	47.525	54.515	66.528	75.982	78.758	81.849
	20	**22.673**	**25.187**	**30.891**	**39.225**	**47.525**	**54.515**	**66.528**	**75.982**	**78.758**	**81.849**
	30	22.673	25.187	30.891	39.225	47.525	54.515	66.528	75.982	78.758	81.849
4.5	10	2.1561	2.5138	3.1959	4.3281	6.0498	6.1521	6.4747	7.0412	7.8963	8.4725
	15	2.1562	2.5139	3.1960	4.3257	6.0501	6.1521	6.4749	7.0416	7.8970	8.4726
	20	**2.1562**	**2.5139**	**3.1960**	**4.3256**	**6.0501**	**6.1522**	**6.4749**	**7.0417**	**7.8971**	**8.4726**
	30	2.1562	2.5139	3.1960	4.3255	6.0501	6.1522	6.4749	7.0417	7.8971	8.4726

5. Conclusions

This research explores the analytical buckling solutions of the thin rectangular plates by adopting the finite integral transform method. The governing high order partial differential equation is converted into a system of a linear algebraic equation, and the analytical solution is obtained elegantly. The main advantage of the proposed method is its simplicity and generality and does not need to pre-determination the deflection function which makes the solving procedure much reasonable. The method can also be extended to bending and vibration as well as thick and moderately thick plate problems. The method can be easy for both engineers and scientists to implement. The present results are believed to provide a benchmark reference for validation of other numerical and analytical methods.

References

Adany, S., Visy, D. and Nagy, R. (2018), "Constrained shell Finite Element Method, Part 2: application to linear buckling analysis of thin-walled members", *Thin-Walled Struct*, **128**, 56–70. https://doi.org/10.1016/j.tws.2017.01.022.

Bui, T.Q. (2011), "Buckling analysis of simply supported composite laminates subjected to an in-plane compression load by a novel mesh-free method", *Vietnam J. Mech.*, **33**(2), 65–78. https://doi.org/10.15625/0866-7136/33/2/39.

Bui, T.Q. and Nguyen, M.N. (2011), "A novel meshfree model for buckling and vibration analysis of rectangular orthotropic plates", *Struct. Eng. Mech.*, **39**(4), 579–598. https://doi.org/10.12989/sem.2011.39.4.579.

Bui, T.Q., Nguyen, M.N. and Zhang, C. (2011), "Buckling analysis of Reissner–Mindlin plates subjected to in-plane edge loads using a shear-locking-free and meshfree method", *Eng. Anal. Bound Elem.*, **35**(9), 1038–1053. https://doi.org/10.1016/j.enganabound.2011.04.001.

Civalek, Ö., Korkmaz, A. and Demir, Ç. (2010), "Discrete singular convolution approach for buckling analysis of rectangular Kirchhoff plates subjected to compressive loads on two-opposite edges", *Adv. Eng. Softw.*, **41**(4), 557–560. https://doi.org/10.1016/j.advengsoft.2009.11.002.

Civalek, O. and Yavas, A. (2008), "Discrete singular convolution for buckling analyses of plates and columns", *Struct. Eng. Mech.*, **29**(3), 279–288. https://doi.org/10.12989/sem.2008.29.3.279.

Ghannadpour, S.A.M. and Ovesy, H.R. (2009), "The application of an exact finite strip to the buckling of symmetrically laminated composite rectangular plates and prismatic plate structures", *Compos. Struct.*, **89**(1), 151–158. https://doi.org/10.1016/j.compstruct.2008.07.014.

Huang, C.S., Lee, H.T., Li, P.Y., Hu, K.C., Lan, C.W. and Chang, M.J. (2019), "Three-dimensional buckling analyses of cracked functionally graded material plates via the MLS-Ritz method", *Thin-Walled Struct*, **134**, 189–202. https://doi.org/10.1016/j.tws.2018.10.005.

Jeyaraj, P. (2013), "Buckling and free vibration behavior of an isotropic plate under nonuniform thermal load", *Int. J. Struct. Stab. Dyn.*, **13**(03), https://doi.org/10.1142/S021945541250071X.

Jiang, L., Wang, Y. and Wang, X. (2008), "Buckling analysis of stiffened circular cylindrical panels using differential quadrature element method", *Thin-Walled Struct.*, **46**(4), 390–398. https://doi.org/10.1016/j.tws.2007.09.004.

Karamooz Ravari, M.R. and Shahidi, A.R. (2013), "Axisymmetric buckling of the circular annular nanoplates using finite difference method", *Meccanica*, **48**(1), 135–144. https://doi.org/10.1007/s11012-012-9589-3.

Karamooz Ravari, M.R., Talebi, S. and Shahidi, A.R. (2014), "Analysis of the buckling of rectangular nanoplates by use of finite-difference method", *Meccanica*, **49**(6), 1443–1455. https://doi.org/10.1007/s11012-014-9917-x.

Komur, M.A. and Sonmez, M. (2015), "Elastic buckling behavior of rectangular plates with holes subjected to partial edge loading", *J. Constr. Steel Res.*, **112**, 54–60. https://doi.org/10.1016/j.jcsr.2015.04.020.

Lau, S. and Hancock, G. (1986), "Buckling of thin flat-walled structures by a spline finite strip method", *Thin-Walled Struct.*, **4**(4), 269–294. https://doi.org/10.1016/0263-8231(86)90034-0.

Li, R., Tian, Y., Wang, P., Shi, Y. and Wang, B. (2016), "New analytic free vibration solutions of rectangular thin plates resting on multiple point supports", *Int J. Mech. Sci.*, **110**, 53–61. https://doi.org/ 10.1016/j.ijmecsci.2016.03.002.

Li, R., Wang, B., Li, G., Du, J. and An, X. (2015), "Analytic free vibration solutions of rectangular thin plates point-supported at a corner", *Int. J. Mech. Sci.*, **96**, 199–205. https://doi.org/ 10.1016/j.ijmecsci.2015.04.004.

Li, R., Wang, B. and Li, P. (2014), "Hamiltonian system-based benchmark bending solutions of rectangular thin plates with a corner point-supported", *Int J. Mech. Sci.*, **85**, 212–218. https://doi.org/ 10.1016/j.ijmecsci.2014.05.004.

Li, R., Zheng, X., Wang, H., Xiong, S., Yan, K. and Li, P. (2018), "New analytic buckling solutions of rectangular thin plates with all edges free", *Int. J. Mech. Sci.*, **144**, 67–73. https://doi.org/10.1016/j.ijmecsci.2018.05.041.

Li, R., Zhong, Y., Tian, B. and Liu, Y. (2009), "On the finite integral transform method for exact bending solutions of fully clamped orthotropic rectangular thin plates", *Appl. Math. Lett.*, **22**(12), 1821–1827. https://doi.org/10.1016/j.aml.2009.07.003.

Lim, C.W., Cui, S. and Yao, W.A. (2007), "On new symplectic elasticity approach for exact bending solutions of rectangular thin plates with two opposite sides simply supported", *Int. J. Solids. Struct*., **44**(16), 5396–5411. https://doi.org/10.1016/j.ijsolstr.2007.01.007.

Lim, C. W., Lü, C. F., Xiang, Y. and Yao, W. (2009), "On new symplectic elasticity approach for exact free vibration solutions of rectangular Kirchhoff plates", *Int. J. Eng. Sci.*, **47**(1), 131–140. https://doi.org/ 10.1016/j.ijengsci.2008.08.003.

Lim, C. W. and Xu, X. S. (2010), "Symplectic elasticity: theory and applications", *Appl. Mech. Rev*., **63**(5), 050802. https://doi.org/10.1115/1.4003700.

Liu, B. and Xing, Y. (2011), "Exact solutions for free vibrations of orthotropic rectangular Mindlin plates", *Compos. Struct*., **93**(7), 1664–1672. https://doi.org/ 10.1016/j.compstruct.2011.01.014.

Liu, B., Xing, Y. F. and Reddy, J. N. (2014), "Exact compact characteristic equations and new results for free vibrations of orthotropic rectangular Mindlin plates", *Compos. Struct*., **118**, 316–321. https://doi.org/ 10.1016/j.compstruct.2014.07.051.

Liu, Y. and Li, R. (2010), "Accurate bending analysis of rectangular plates with two adjacent edges free and the others clamped or simply supported based on new symplectic approach", *Appl. Math. Model*., **34**(4), 856–865. https://doi.org/10.1016/j.apm.2009.07.003.

Mahendran, M. and Murray, N. (1986), "Elastic buckling analysis of ideal thin-walled structures under combined loading using a finite strip method", *Thin-Walled Struct*., **4**(5), 329–362. https://doi.org/10.1016/0263-8231(86)90029-7.

Mijušković, O., Ćorić, B. and Šćepanović, B. (2015), "Accurate buckling loads of plates with different boundary conditions under arbitrary edge compression", *Int. J. Mech. Sci*., **101**, 309–323. https://doi.org/ 10.1016/j.ijmecsci.2015.07.017.

Ovesy, H. R., Ghannadpour, S. A. M. and Zia-Dehkordi, E. (2013), "Buckling analysis of moderately thick composite plates and plate structures using an exact finite strip", *Compos. Struct*., **95**, 697–704. https://doi.org/10.1016/j.compstruct.2012.08.009.

Simulia, D. S. (2013). "Abaqus 6.13 Analysis User's Guide." Dassault Systems, Providence, RI, USA.

Singhatanadgid, P. and Taranajetsada, P. (2016), "Vibration analysis of stepped rectangular plates using the extended Kantorovich method", *Mech. Adv. Mater. Struct*., **23**(2), 201–215. https://doi.org/ 10.1080/15376494.2014.949922.

Tian, B., Li, R. and Zhong, Y. (2015), "Integral transform solutions to the bending problems of moderately thick rectangular plates with all edges free resting on elastic foundations", *Appl. Math. Model*., **39**(1), 128–136. https://doi.org/ 10.1016/j.apm.2014.05.012.

Tian, B., Zhong, Y. and Li, R. (2011), "Analytic bending solutions of rectangular cantilever thin plates", *Arch. Civ. Mech. Eng*., **11**(4), 1043–1052. https://doi.org/ 10.1016/S1644-9665(12)60094-6.

Timoshenko, S.P. (1961). *Theory of Elastic Stability Second Edition*. McGraw-Hill Book Company, Inc., New York, USA.

Ullah, S., Zhong, Y. and Zhang, J. (2019), "Analytical buckling solutions of rectangular thin plates by straightforward generalized integral transform method", *Int. J. Mech. Sci*., **152**, 535–544. https://doi.org/10.1016/j.ijmecsci.2019.01.025.

Wang, B., Li, P. and Li, R. (2016), "Symplectic superposition method for new analytic buckling solutions of rectangular thin plates", *Int. J. Mech. Sci*., **119**, 432–441. https://doi.org/10.1016/j.ijmecsci.2016.11.006.

Wang, J., Liew, K. M., Tan, M. J. and Rajendran, S. (2002), "Analysis of rectangular laminated composite plates via FSDT meshless method", *Int. J. Mech. Sci*., **44**(7), 1275–1293. https://doi.org/ 10.1016/S0020-7403(02)00057-7.

Wang, X. and Huang, J. (2009), "Elastoplastic buckling analyses of rectangular plates under biaxial loadings by the differential qudrature method", *Thin-Walled Struct*., **47**(1), 14–20. https://doi.org/10.1016/j.tws.2008.04.006.

Wang, X., Tan, M. and Zhou, Y. (2003), "Buckling analyses of anisotropic plates and isotropic skew plates by the new version differential quadrature method", *Thin-Walled Struct*., **41**(1), 15–29. https://doi.org/10.1016/S0263-8231(02)00100-3.

Wu, C.P. and Lin, H.R. (2015), "Three-dimensional dynamic responses of carbon nanotube–reinforced composite plates with surface-bonded piezoelectric layers using Reissner's mixed variational theorem–based finite layer methods", *J. Intell. Mater. Syst. Struct*., **26**(3), 260–279. https://doi.org/ 10.1177/1045389X14523859.

Xiang, Y., Wang, C.M. and Kitipornchai, S. (2003), "Exact buckling solutions for rectangular plates under intermediate and end uniaxial loads", *J. Eng. Mech*., **129**(7), 835–838. https://doi.org/ 10.1061/(ASCE)0733-9399(2003)129:7(835).

Xing, Y.F. and Liu, B. (2009), "New exact solutions for free vibrations of thin orthotropic rectangular plates", *Compos. Struct*., **89**(4), 567–574. https://doi.org/10.1016/j.compstruct.2008.11.010.

Yufeng, X. and Wang, Z. (2017), "Closed form solutions for thermal buckling of functionally graded rectangular thin plates", *Appl. Sci*., **7**(12), 1256. https://doi.org/10.3390/app7121256.

Zhang, J., Zhou, C., Ullah, S., Zhong, Y. and Li, R. (2018), "Two-dimensional generalized finite integral transform method for new analytic bending solutions of orthotropic rectangular thin foundation plates", *Appl. Math. Lett*., **92**, 8-14. https://doi.org/ 10.1016/j.aml.2018.12.019.

Zhang, S. and Xu, L. (2018), "Analytical solutions for flexure of rectangular orthotropic plates with opposite rotationally restrained and free edges", *Arch. Civ. Mech. Eng.,* **18**(3), 965–972. https://doi.org/10.1016/j.acme.2018.02.005.

Zhang, S. and Xu, L. (2017), "Bending of rectangular orthotropic thin plates with rotationally restrained edges: A finite integral transform solution", *Appl. Math. Model*., **46**, 48–62. https://doi.org/ 10.1016/j.apm.2017.01.053.

Zhang, Y. and Zhang, S. (2018), "Free transverse vibration of rectangular orthotropic plates with two opposite edges rotationally restrained and remaining others free", *Appl. Sci*., **9**(1), 22. https://doi.org/10.3390/app9010022.

Zhong, Y. and Yin, J.H. (2008), "Free vibration analysis of a plate on foundation with completely free boundary by finite integral transform method", *Mech. Res. Commun*., **35**(4), 268–275. https://doi.org/ 10.1016/j.mechrescom.2008.01.004.

Zhong, Y., Zhao, X. and Liu, H. (2014), "Vibration of plate on foundation with four edges free by finite cosine integral transform method", *Lat. Am. J. Solids Struct*., **11**(5), 854–863. https://doi.org/10.1590/S1679-78252014000500008.

Zhou, D., Cheung, Y.K. and Kong, J. (2000), "Free vibration of thick, layered rectangular plates with point supports by finite layer method", *Int. J. Solids Struct*., **37**(10), 1483-1499. https://doi.org/ 10.1016/S0020-7683(98)00316-3.

PL